

Article

Potential of Biochar Derived from Agricultural Residues for Sustainable Management

Sasiwimol Khawkomol ¹, Rattikan Neamchan ², Thunchanok Thongsamer ³, Soydoa Vinitnantharat ^{2,3,*} , Boonma Panpradit ^{1,4}, Prapa Sohsalam ⁵, David Werner ⁶ and Wojciech Mroziak ⁶

- ¹ Energy and Environmental Engineering Center, Faculty of Engineering at Kamphaeng Saen, Kasetsart University, Nakhon Pathom 73140, Thailand; sasiwimol.kh@ku.ac.th (S.K.); fengbop@ku.ac.th (B.P.)
- ² Environmental and Energy Management for Community and Circular Economy (EE&C) Research Group, King Mongkut's University of Technology Thonburi, Bangkok 10140, Thailand; r.neamchan@gmail.com
- ³ Environmental Technology Program, School of Energy, Environment and Materials, King Mongkut's University of Technology Thonburi, Bangkok 10140, Thailand; thunchanok.t@mail.kmutt.ac.th
- ⁴ Department of Irrigation Engineering, Faculty of Engineering at Kamphaeng Saen, Kasetsart University, Nakhon Pathom 73140, Thailand
- ⁵ Faculty of Liberal Arts and Science at Kamphaeng Saen, Kasetsart University, Nakhon Pathom 73140, Thailand; faaspps@ku.ac.th
- ⁶ School of Engineering, Newcastle University, Newcastle upon Tyne NE1 7RU, UK; david.werner@newcastle.ac.uk (D.W.); wojciech.mroziak@newcastle.ac.uk (W.M.)
- * Correspondence: soydoa.vin@mail.kmutt.ac.th; Tel.: +66-2-470-8673



Citation: Khawkomol, S.; Neamchan, R.; Thongsamer, T.; Vinitnantharat, S.; Panpradit, B.; Sohsalam, P.; Werner, D.; Mroziak, W. Potential of Biochar Derived from Agricultural Residues for Sustainable Management. *Sustainability* **2021**, *13*, 8147. <https://doi.org/10.3390/su13158147>

Academic Editors: Keiji Jindo and Hans Langeveld

Received: 24 May 2021

Accepted: 19 July 2021

Published: 21 July 2021

Publisher's Note: MDPI stays neutral with regard to jurisdictional claims in published maps and institutional affiliations.



Copyright: © 2021 by the authors. Licensee MDPI, Basel, Switzerland. This article is an open access article distributed under the terms and conditions of the Creative Commons Attribution (CC BY) license (<https://creativecommons.org/licenses/by/4.0/>).

Abstract: A horizontal drum kiln is a traditional method widely used in Southeast Asian countries for producing biochar. An understanding of temperature conditions in the kiln and its influence on biochar properties is crucial for identifying suitable biochar applications. In this study, four agricultural residues (corn cob, coconut husk, coconut shell, and rice straw) were used for drum kiln biochar production. The agricultural residues were turned into biochar within 100–200 min, depending on their structures. The suitability of biochar for briquette fuels was analyzed using proximate, ultimate, and elemental analysis. The biochar's physical and chemical properties were characterized via bulk density, iodine number, pH_{pzc} , SEM, and FTIR measurements. All biochars had low O/C and H/C ratios and negative charge from both carbonyl and hydroxyl groups. Coconut husk and shell biochar had desirable properties such as high heating value and a high amount of surface functional groups which can interact with nutrients in soil. These biochars are thus suitable for use for a variety of purposes including as biofuels, adsorbents, and as soil amendments.

Keywords: agricultural residues; biochar; biochar characterization; biochar application

1. Introduction

Agriculture is one of the dominant sectors for both the Thai economy and other South-east Asian (SEA) countries, with a high overseas demand for their food and agricultural products such as rice, sugar, coconut, and corn. Consequently, these countries produce high amounts of agricultural residues from both harvesting and the food processing industries. It was estimated that there more than 500 million tons/year of residues are produced from the agricultural and forest sectors of SEA countries [1]. Thus, these residues represent a significant challenge to proper waste management and reuse. The conversion of these agricultural residues into biochar represents a promising avenue for their reuse and valorization. Biochar is a carbon-rich material which is mostly derived from biomass and has high stability in the environment.

It has been widely reported that biochar can be used directly as a renewable energy source [2], as a soil amendment to improve fertility [3] and control soil greenhouse gas emission [4,5], and as a filter media for wastewater treatment [6]. The process of making biochar produces less air pollution than the open burning of agricultural residues in fields,

which can emit noxious gases (CO, SO_x, NO_x) and smoke particles carrying carcinogen substances [7]. Apart from the particulate matter, a 16 polyaromatic hydrocarbon concentration ranging between 151.7 and 1090.4 µg/m³ was reported from the open burning of agricultural debris in fields [8], which has adverse health effects.

The thermal conversion of biomass into biochar depends on both temperature and the amount of oxygen present. The processes involved include drying, torrefaction, carbonization, pyrolysis, gasification, and combustion [9]. There are many reactors for the production of biochar and heating systems including combustion, electricity, induction, microwave or solar heating through an external diaphragm, and inert gas or sand. The shape of reactors is typically cylindrical, conical, or cuboid [9]. A cylindrical reactor can be made from 200 L oil drums placed in horizontal, vertical, or oblique position. Other types of traditional kilns widely used in Asian countries include earth-mound kilns and brick kilns, since they require low investment and are made of easy to find construction materials. Earth-mound kilns or pit kilns are constructed by digging a hole, laying the biomass in the pit, and covering it with soil which is used in small-scale conservation agriculture [10]. This low technology kiln is commonly used in rural areas. However, while the quality of the charcoal is good in these cases, the energy loss is greater than that of other kilns. Brick kilns are typically used in industrial applications, as they need to produce more biochar than other types of kilns in order to recover the higher cost of construction. Their furnace life is long, and one can easily control the temperature during the brick kiln combustion process. However, brick kilns cannot be moved. Drum kilns are very popular in the rural areas of Thailand as they are more efficient than other traditional kilns. Drum kilns enable control of inlet air during carbonization. The produced charcoal is of high quality and contains less ash. Moreover, there are byproducts from the charcoal production process (namely wood vinegar or tar). The charcoal can be used as pest control and to produce liquid fertilizer [11]. The drum kiln service life is between two and three years. The simple design of horizontal drum kilns makes it possible for rural people in Thailand and other SEA countries to make the kiln themselves and produce biochar for their uses in households and for commercial purposes. However, the biochar's characteristics vary for different biomass starting materials [12], pyrolysis temperatures, and pyrolysis conditions [13]. The chemical and physical characteristics of biochar are crucial sources of information for selecting the best valorization pathway. Biochar is currently being used as soil amendment for the enhancement of nutrient fertility in soil. Recently, many researchers have also investigated the use of biochar derived from agricultural residues for the removal of organic substances, metals, nutrients, and pathogens as an environmentally low-cost adsorbent and locally available material. Most tests have been conducted in aqueous solution using a batch experiment. Water filtration trials have been conducted using biochar either solely or incorporated with sand. Biochar technology is popular in developing countries for household uses including energy and food security and also water purification [14]. Biochar is also currently used for briquette making as an alternative fuel in rural area since it has higher calorific value than raw biomass [15]. The suitable fuel properties are normally determined by proximate analysis (contents of moisture, ash, volatile matter, and fixed carbon). Agricultural residues in Thailand are ubiquitous, particularly rice and corn residues [16], whereas coconut residue is available in the coastal and central areas of Thailand. Thus, they are available locally for the production of biochar. The aims of this paper are: (i) to produce biochar from four common agricultural residues, corncob (CC), coconut husk (CH), coconut shell (CS), and rice straw (RS) using a horizontal drum kiln method; (ii) to investigate the physical and chemical properties of biochar for its potential use as adsorbent and soil amendment; (iii) to identify the most suitable biochars for fuel use; and (iv) to evaluate the use of biochar for canal water filtration and seed germination.

2. Materials and Methods

2.1. Agricultural Residues and Biochar Preparation

Four common agricultural residues in central Thailand, namely CC, CS, CH, and RS were used in this study. CC was obtained from a local market and was sun dried. The rest were obtained from the fields and used as received. A horizontal drum kiln with a capacity of 0.2 m³ at the Center for Energy and Environmental Engineering, Kasetsart University, Kamphaeng Saen campus, was used to produce the biochar. The chimney was welded onto the bottom of the drum. The drum kiln was first placed in a rectangular foundation made by a concrete block. Then, the entire drum was covered with sand to prevent heat loss during carbonization. Figure 1 shows the front view and side view of the drum and connected pipes. A thermocouple was installed at 20 cm depth from the drum wall to monitor the temperature inside the chamber every 10 min from the start up to 600 min. The CC, CH, CS, and RS residues with a dry weight of 18.4, 10.4, 34, and 10 kg, respectively, were loaded into the chamber of the drum kiln. The loaded drum's lid was closed and sealed with clay or mortar, except for the firing section. Small pieces of wood were stacked in the firing section to light the kiln. More wood pieces were placed into the firing section to burn until smoke was observed coming out through the chimney. White smoke was released from the chimney while the agricultural residues were partially decomposed with the release of water vapor. Air intake was then reduced by covering the front aeration channel to about one fourth and the smoke became clear. This showed that the agricultural residue was fully carbonized. The firing section was completely closed with clay and the chimney was also sealed. The sealed kiln was then left overnight for at least 12–15 h to complete the biochar production process. The biochar was weighed and the percentage of yield was determined as the ratio of the biochar mass to raw biomass. After cooling, all biochar samples were ground to less than 2 mm in diameter.

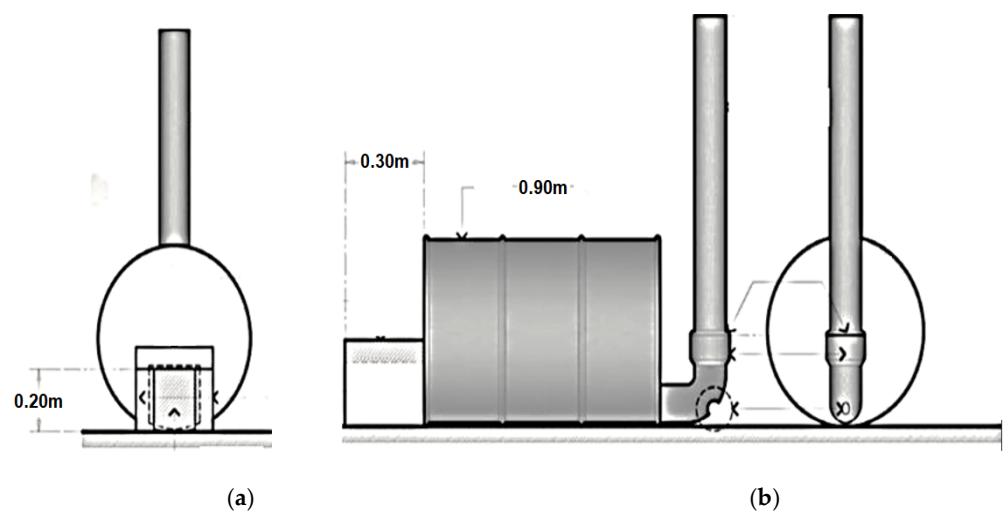


Figure 1. Schematic of the horizontal drum kiln pyrolysis unit. (a) Front view and (b) side view.

2.2. Biochar Characterization

The morphological surfaces of biochar were observed by scanning electron microscopy (Hitachi, SU-1000, Chiyoda City, Tokyo, Japan). Bulk density ($d = m/V$) was measured using the mass of dry sample (m) and total volume of sample (V) [17], where total volume considers both the solid and pore space. Surface areas of the biochars were determined by N₂-adsorption based techniques (Brunauer–Emmett–Teller, BET surface area) which is normally applicable for non-porous samples as well as for samples having pores in the meso- and macro range. The iodine number was measured as a relative indicator of porosity following method ASTM D4607 [18].

Characterization of biochars by proximate analysis was used to determine moisture, ash, volatile matter, and fixed carbon following the methods ASTM D3173, ASTM D3174,

and ASTM D3175, respectively [19]. The percentage of fixed carbon was computed by subtracting the sum of moisture content, ash content, and volatile matter from 100. The ultimate analysis was carried out to determine the percentage of carbon, hydrogen, nitrogen and sulfur elements using a Perkin Elmer 2400-II CHNS/O elemental analyzer. The oxygen content was calculated by difference. The heating value of the biochars was measured using a bomb calorimeter (Parr 6400 automatic isoperibol calorimeter).

Metals of biochar samples were characterized by X-ray fluorescence (XRF) with a Bruker AXS S4 Pioneer instrument. To investigate the functional groups of the biochars, samples were mixed with KBr and the mixture was ground and characterized by Fourier transform-infrared (FTIR) spectroscopy with a Nicolet 6700 spectrometer (Thermo Scientific, Waltham, MA, USA). The spectrum was scanned over the wavelength number range between 600 cm^{-1} to 4000 cm^{-1} .

The pH of solution (pH_{sol}) of the biochar samples was analyzed by placing the biochar in deionized water at a ratio of 1:10 (w/v). The mixture was shaken at 100 rpm at $30\text{ }^{\circ}\text{C}$ for 3 h, then the pH was recorded using a pH meter. The pH at the point of zero charge (pH_{pzc}) was analyzed using the pH drift method. Biochar (0.15 g) was added into 50 mL of 0.01N NaCl solution with different pH values of 1.0, 3.0, 5.0, 7.0, 9.0, and 11.0, adjusted using NaOH or HCl. The mixture at each initial pH was shaken at 100 rpm and $30\text{ }^{\circ}\text{C}$ for 48 h prior to pH measurement. The initial pH and final pH was plotted to determine the pH_{pzc} at which the initial pH equals the final pH.

Ions released from each biochar were investigated by a method modified from Yuan et al. [20]. Biochar at 5 g was leached with 50 mL deionized water by shaking at 100 rpm, at $30\text{ }^{\circ}\text{C}$ for 3 h. The solution was filtered and the cations and anions were analyzed by ion chromatography (761 Compact IC, Metrohm; column Metrosep A Supp5-150/4.0 at flow rate of 0.6 mL/min and Metrosep C4-100/4.0 at flow rate of 0.9 mL/min). The sum of potassium (K^+), sodium (Na^+), calcium (Ca^{2+}) and magnesium (Mg^{2+}) ions was calculated as the soluble base cations of the biochar. Soluble nitrogen (N) represented nitrogen in the form of ammonium (NH_4^+) + nitrate (NO_3^-), and soluble phosphorus (P) represented PO_4^{3-} in the leachate.

2.3. Biochar for Water Filtration and Seed Germination Study

CH biochar was selected to study its application for water filtration and then phytotoxicity test. Cylindrical-shaped columns with a 0.525 L volume were used for studying the nutrient and chemical oxygen demand (COD) removal from canal water with this biochar, compared to a sand filter. The bed height was 13.2 cm and the column diameter was 5.8 cm. A biochar mass of 0.1 kg was placed in the column and soaked with deionized water for 3 days. Then, canal water from near an aquaculture farm was fed continuously with a downward flow at a rate of 15 mL/min for 420 min. The effluent was collected at intervals over a period of time and analyzed for pH, NH_4^+ , NO_3^- , total phosphorus (TP) and COD following standard methods for the examination of water and wastewater [21].

The phytotoxicity test was adapted from Tiquia [22] to test for an eventual toxic effect of leachates from sand and biochar on plant germination. Biochar and sand before and after water filtration were extracted with DI water for a biochar dosage of 10% (w/v) after contact at $30\text{ }^{\circ}\text{C}$ and 100 rpm for 1 h. The extracted solution was filtered through a $0.45\text{ }\mu\text{m}$ membrane. Then, 20 seeds of Pak Choi were placed in 5 mL of the extract solution and DI water was used as a control in the petri dish. All petri dishes were covered with lids and left for five days in the dark at room temperature. The number of seeds germinated and root length for each solution were measured. Calculation of the relative seed germination (RSG), relative elongation (RE), and germination index (GI) followed Equations (1)–(3).

$$\text{RSG (\%)} = 100(\text{A/B}) \quad (1)$$

$$\text{RE (\%)} = 100(\text{C/D}) \quad (2)$$

$$\text{GI (\%)} = (\text{RSG} \times \text{RE})/100 \quad (3)$$

where A and B are the number of seeds germinated in extracted solution and in DI water, respectively. C and D are the mean length of root in each solution.

3. Results and Discussion

3.1. Temperature Profile and Yield

During carbonization, the temperature as a function of time of heating was monitored to find out the maximum temperature for each agricultural residue turned into biochar. This present paper is, to the best of our knowledge, the first paper reporting the temperature profile for biochar making in a drum kiln, as far as non-rotary drum kilns are concerned. The heat transfer profiling was previously done only for the rotary one [23]. The temperature inside the kiln rose up to a peak and then decreased due to the evaporation of water and volatile matter during thermal decomposition (Figure 2). Pyrolysis took place over the temperature range between 150 and 400 °C, when lignin would be decomposed and gaseous products formed such as H₂, CO, and CO₂ [24]. Acids, ketones, phenols, guanidines, and furans would be formed for temperatures between 400 and 700 °C [9]. Lian and Xing [25] also reported that the molecular structure of biochar is completed when reaching 700 °C. The peak temperature and the time taken to reach the maximum temperature of each agricultural residue were variable due to the different chemical composition of the plant fibers. Maximum temperatures of 480, 378, 704, and 303 °C were reached for CC, CH, CS, and RS, respectively, after carbonization for 100–200 min. The maximum peaks were either sharp (CC and CH) or broad shaped (CS and RS), which then tailed off after the maximum peak.

CH gave the highest biochar yield (33.7%), followed by CC (32.0%), CS (23.8%), and RS (10.0%). The low yield of RS is due to a lower amount of fixed carbon and high amount of inorganic materials compared to the other agricultural residues. The loss of weight from thermal conversion of biomass to char is related to: (1) dehydration, decomposition, and dehydroxylation of carbonates, sulfates, hydroxides and silicates; (2) oxidation of sulfide and hydration and hydroxylation of some oxides; and (3) melt evaporation [26].

3.2. Physical Characteristic of Biochars

The structures of biochar presented in Figure 3 show the numerous hollow channels, mostly with diameters of less than 20 micron. The International Union of Pure and Applied Chemistry (IUPAC) classifies the pore sizes into 3 classes, micropore (<2 nm), mesopore (2–50 nm) and macropore (>50 nm).

Bulk density of CC, CH, CS, and RS biochars were 0.69, 0.66, 1.14, and 1.69 g/cm³, respectively. Those biochars which have a bulk density lower than 1.00 will float in both water and soil solutions. BET surface areas of CH and RS biochars were low at 11.0 and 14.6 m²/g, respectively. Biochar without surface modification derived from the pyrolysis of cashew nuts was also reported to have a low BET surface area of 0.8 m²/g. The BET surface area increased to 9 and 13 m²/g when it was activated with steam and carbon dioxide at temperatures of 600 °C and 650 °C, respectively [27]. BET surface areas could not be established for corncob and coconut shell biochars. Low BET surface areas are attributed to the clogging of pores from the condensation of organic volatiles after pyrolysis [28]. Nitrogen gas is generally employed as the probe molecule in BET surface analysis since it is a small molecule which can penetrate into the mesopores (2–50 nm). Iodine number is normally correlated with micropore volume and is relative to pores with a 0.1–0.3 nm diameter (Iodine atomic radius = 0.132 nm). Adsorption of iodine in aqueous solution forms a unimolecular layer on the surface, but adsorption from vapor forms pore filling in micropores and then surface coverage in macropores [29,30]. It was found that iodine numbers of CC, CH, CS, and RS biochars were 32.3, 68.4, 13.2, and 3.06 mg/g, respectively. All biochars contain meso and micropores. Hence, this gives biochars a good property for soil amendment to improve water holding capacity, soil aeration, microbial attachment, and pollutant adsorption, particularly for the coconut husk biochar.

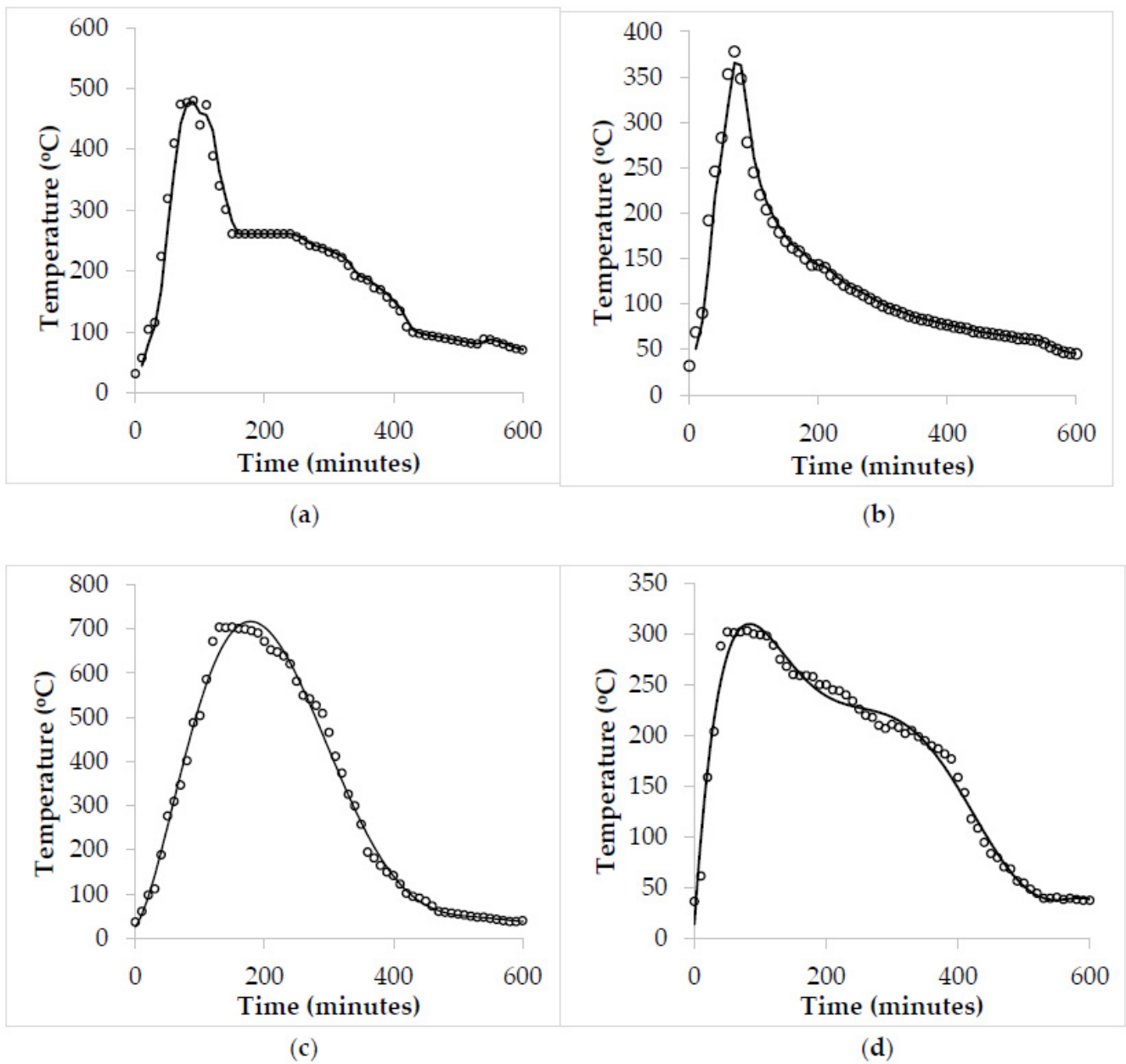


Figure 2. Temperature in the oil drum kiln: (a) corncob; (b) coconut husk; (c) coconut shell; and (d) rice straw.

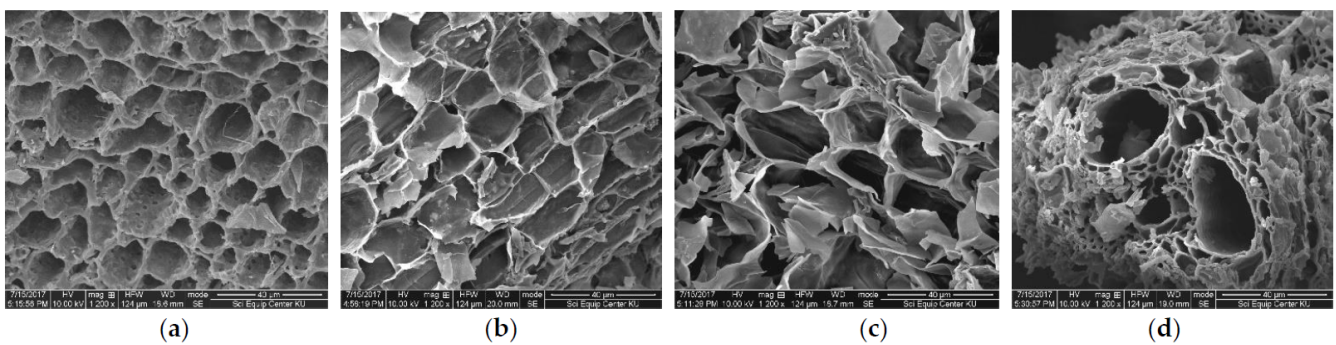


Figure 3. SEM images of the biochars ($\times 1200$ magnification): (a) corncob; (b) coconut husk; (c) coconut shell; and (d) rice straw.

3.3. Chemical Characteristics of Biochars

The FTIR spectra of biochar are presented in Figure 4. According to the results of Jouiad et al. [28], the bands assigned to O–H stretching ($3200\text{--}3000\text{ cm}^{-1}$) and C–H stretching ($3100\text{--}3000\text{ cm}^{-1}$) correspond to hemicellulose and cellulose, and the bands in the $900\text{--}1400\text{ cm}^{-1}$ range are representative of lignin. The mentioned band for hemicellulose and cellulose were absent in all biochar samples due to the decomposition of the raw biomass. A relatively small peak was found at 1362 cm^{-1} for CH biochar indicative of lignin (C–O group of carboxyl and alcohol). Broad bands at 1050 and 787 cm^{-1} were found in RS biochar due to the stretching of C–O–C and Si–O–Si groups, respectively. These peaks existed as there were strong chemical bonds [31]. The band intensity in the 1600 cm^{-1} region appeared indicative of conjugated C=C phenyl rings of ketones and quinones. This implies condensation of the biochar organic compounds which is in agreement with the results reported by other researchers [32–34]. Peaks for C–H bending bonds (out of plane) in the region of $900\text{--}675\text{ cm}^{-1}$, which are characteristic of the aromatic substitution pattern, were clearly visible for all biochars except for a small peak for the corncob biochar. Thus, the functional groups associated with the biochar surfaces were negative charges, with carbonyl and hydroxyl groups attached to highly aromatic structures. RS biochar also contained negative charges from silica. The highly negative surface charge of biochar gives it potential for heavy metal adsorption through various mechanisms such as cation exchange, electrostatic interactions, complexation, and precipitation onto biochar surfaces [35].

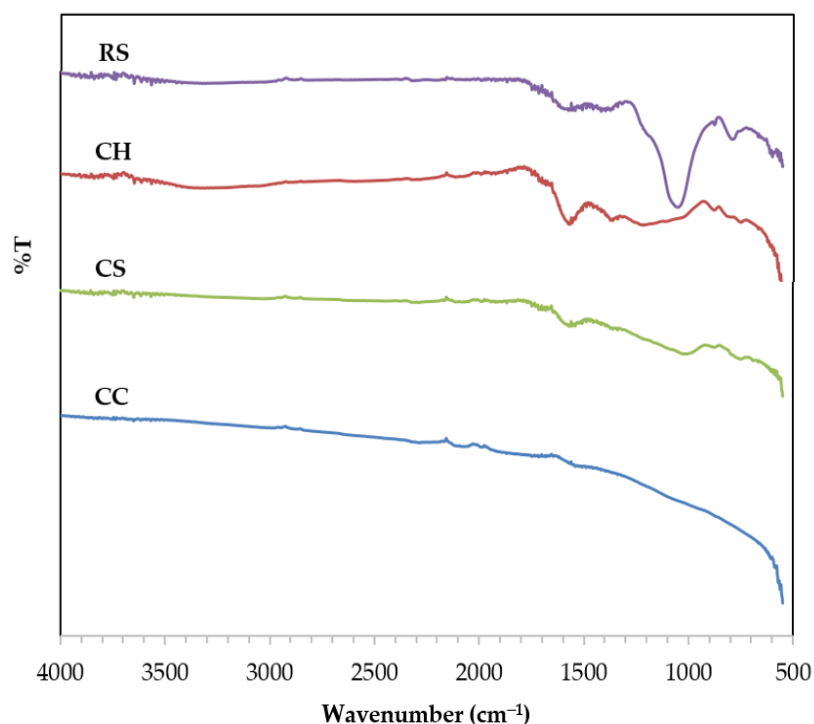


Figure 4. FTIR spectra of the biochars.

All biochar samples had high pH with an average of 9.17, at which most heavy metals can be precipitated (Table 1). However, the surface charge of biochars is pH dependent. In general, if pH_{sol} is $< \text{pH}_{\text{pzc}}$, the surface charge of biochars exhibit a positive charge due to the protonation of the acidic groups. This will decrease the adsorption of heavy metals due to the electrostatic repulsion between surface positive charges and heavy metal ions. On the contrary, when pH_{sol} is $> \text{pH}_{\text{pzc}}$, the surface functional groups are deprotonated and are favorable to adsorb heavy metal and cationic ions such as ammonium. In this present study, all biochars exhibited negative surface charges.

Table 1. Chemical characteristics of the biochars.

| Biochar | pH _{sol} | pH _{pzc} | Soluble (mmol/g) | | | | Metal (% by Weight) | | | | | | | | | |
|---------|-------------------|-------------------|------------------|------|------|------|---------------------|------|------|------|------|------|------|------|------|--|
| | | | Base Cation | N | P | K | Na | Ca | Mg | Fe | Zn | Al | Si | Cl | P | |
| CC | 8.97 | 8.61 | 652 | 0.28 | 9.45 | 15 | 4.38 | 3.43 | 1.60 | 0.26 | 0.35 | 0.06 | 5.27 | 19.5 | 2.71 | |
| CH | 9.75 | 9.39 | 1027 | 0.59 | 6.27 | 23.9 | 1.92 | 6.91 | 1.46 | 0.49 | 0.03 | 0.10 | 3.36 | 14.6 | 0.60 | |
| CS | 9.02 | 8.53 | 77 | 0.41 | 1.21 | 8.84 | 0.56 | 3.04 | 1.38 | 3.39 | 0.07 | 1.92 | 20.8 | 0.96 | 0.90 | |
| RS | 8.94 | 8.88 | 1543 | 0.60 | 3.52 | 6.68 | 1.50 | 5.09 | 2.29 | 0.76 | 0.01 | 0.06 | 24.9 | 9.45 | 0.63 | |

Note: pH_{sol} = 5 g biochar in 50 mL deionized water at 100 rpm, 30 °C for 3 h; pH_{pzc} = 0.15 g biochar in 50 mL 0.01 N NaCl at 100 rpm, 30 °C for 48 h; Base cation = K⁺ + Na⁺ + Ca²⁺ + Mg²⁺; Soluble N = NH₄⁺ + NO₃⁻.

Results from metal analysis revealed that biochar derived from rice straw and coconut shells contained high amounts of silica and potassium, whereas potassium and chloride were the main inorganic components in CH and CC biochars (Table 1). This finding corresponds with previous research, reporting high silica and potassium for agricultural residues from straw [36]. The sequences of metals follow K > Cl > Si > Na > Ca, K > Cl > Ca > Si > Na, Si > K > Fe > Ca > Al and Si > K > Cl > Ca > Mg for CC, CH, CS, and RS, respectively. Potassium, calcium, magnesium, and sodium are all water soluble, making the biochars alkalic. Biochars can release ions as they have high soluble base cations, particularly for rice straw and coconut husk biochars. They also can release nitrogen (NH₄⁺ + NO₃⁻) and phosphorus. Thus, biochar amendment in soil can enhance soil fertility through improving nutrient availability for both macronutrients (N, P, K, Ca and Mg) and micronutrients (Fe and Zn). RS and CS biochar have high silica contents which benefit plant growth. Silica enhances the crop productivity under stress as the chemical dynamics between Si and many soil components enhances nutrient availability and decrease toxic chemical availability in both soils and plants [37]. The application of RS biochar was reported to immobilize and reduce lead and cadmium in soil [38].

3.4. Proximate and Ultimate Analysis

Proximate analysis is normally used to determine the properties of biochar for fuel use. The biochar from CC had the highest moisture and volatile matter content (Table 2). High volatile matter can increase the heating value, but high moisture is undesirable in fuel. It requires time and energy to change the moisture into vapor, subsequently increasing cost. Biochar from RS had the lowest high heating value (HHV) (14.24 MJ/kg) because of its high content of ash (35.75%). CH and CS have better HHVs as they have high fixed carbon and low ash. This proximate analysis result was similar to the work performed by Gonzaga et al. [39] for coconut husk biochar produced using pyrolysis in a micro top-lit updraft retort at 500 °C.

Table 2. Proximate analysis and heating value of the produced biochars.

| Biochar | Moisture (%) | Ash (%) | Volatile Matter (%) | Fixed Carbon (%) | High Heating Value (MJ/kg) |
|---------|--------------|---------|---------------------|------------------|----------------------------|
| CC | 18.67 | 6.33 | 48.97 | 26.03 | 22.05 |
| CH | 1.69 | 8.56 | 5.99 | 83.76 | 23.26 |
| CS | 2.96 | 4.42 | 38.63 | 53.99 | 23.60 |
| RS | 1.91 | 35.75 | 33.41 | 28.93 | 14.24 |

In the present study, the CS-based biochar comprised more volatile matter but less fixed carbon than the biochar from CH. Wang and Sarkar [40] reported that CH and CS contain high cellulose and lignin, with the shell having the highest amount of cellulose and husk the maximum amount of lignin. The higher cellulose content of the shell produced more tar than the husk. It was also reported that higher lignin content in biomass increases HHV [41]. Cellulose and hemicelluloses were reported to have HHVs of 18.60 MJ/kg, whereas lignin has an HHV of 23.26–25.58 MJ/kg [42]. At temperatures below 300 °C,

dehydration and depolymerization of cellulose occurred via torrefaction, subsequently becoming hydrophobic [9]. Thus, RS was transformed into a torrefied biomass rather than char as the entire temperature during thermal decomposition was less than 300 °C. As temperature increases, the thermal decomposition continues, resulting in liquid or gaseous products and a decrease in the ratios of O/C and H/C.

The results of ultimate analysis (elemental C, H, N, S and O) of raw biomass and biochar samples are represented in Figure 5. It was revealed that biochars became more carbonaceous with the percentage of carbon ranging between 53.6 and 68.6%. From the percentage of each element, the molecular formula of the raw biomass samples were CH_2O , $\text{CH}_{1.5}\text{O}_{0.8}$, $\text{CH}_{1.6}\text{O}_{0.6}$, and $\text{CH}_2\text{O}_{0.6}$ for CC, CH, CS, and RS, respectively. Then, the loss of hydrogen and oxygen during thermal conversion changed these molecular formulas to $\text{CH}_{0.6}\text{O}_{0.4}$, $\text{CH}_{0.6}\text{O}_{0.3}$, $\text{CH}_{0.6}\text{O}_{0.3}$, and $\text{CH}_{0.6}\text{O}_{0.6}$ for CC, CH, CS, and RS biochars, respectively. All biochar samples had lower H/C and O/C ratios than their parent raw biomass because of the loss of carbon and hydrogen into gases. Cellulose is the main structural component of cell walls and a linear molecule; hemicellulose is a two dimensional polymer molecule of xylan and glucomannan; and lignin is a three-dimensional macromolecule. There are hydrogen bonding and van der Waals forces among cellulose, hemicellulose, and lignin molecules [43]. During thermal conversion, various atoms form new bonds in new molecules of carbon dioxide, water, and other gases, and the formation of new bonds is an exothermic process in which heat is given off. The bond energy of C=O (CO_2) is 803 kJ/mol. The O/C ratio decreased around 60% for corncob and coconut husk to biochars resulting in O/C ratios of 0.3. The low ratios indicate that the biochars have better fuel characteristics than the raw biomass. The O/C ratios of rice straw biochar was the highest at 0.6, resulting in the lowest heating value. In addition, biochars produced at higher temperatures have lower O/C ratio, and the ratio correlates with high heating value [36,44]. The European Biochar Certificate (EBC) includes requirements that the molar ratios of O/C and H/C should be less than 0.4 and 0.7, respectively [45].

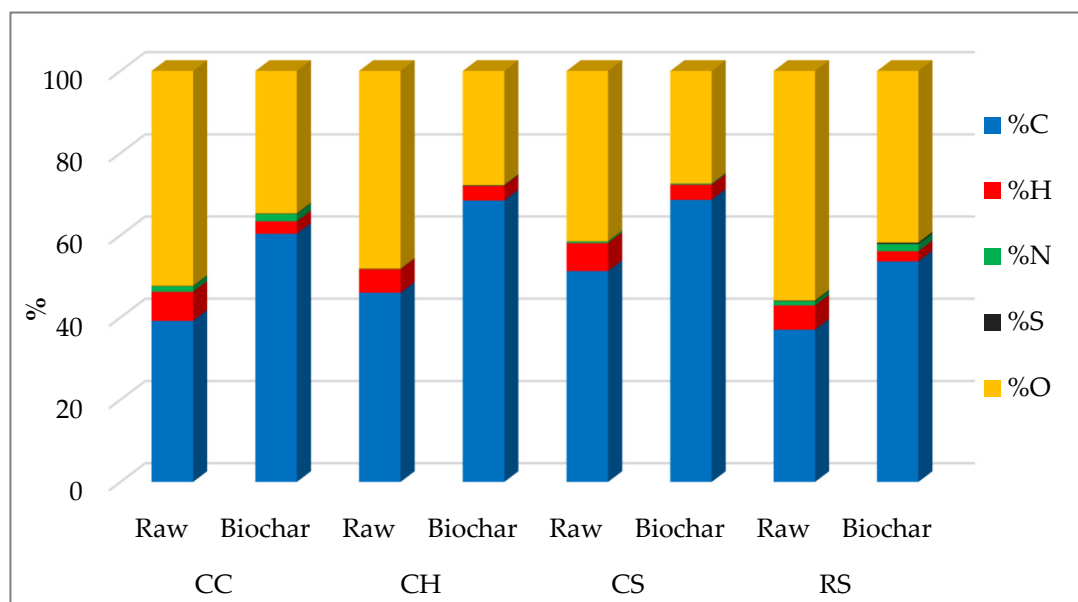


Figure 5. Ultimate analysis of the biochars.

Recently, biochar was used solely or mixed with biomass in the form of pellets [2] or briquettes to increase HHV of fuel for households and small-scale factories. Starch or molasses are binding materials normally applied to make pellets or briquettes from biochar. The Thai standard for community briquette charcoal mandates that the HHV is no less than 21 MJ/kg and the maximum moisture content should be no more than 8% [46]. From this present study, CH and CS biochars have the potential to make pellet and briquette fuel.

The RS biochar did not meet the requirement of the EBC certificate ($O/C > 0.4$) and Thai standard ($HHV < 21 \text{ MJ/kg}$), whereas while the CC biochar contained higher moisture than the Thai standard the ash content was too high. High ash content of fuel has a tendency to form slag deposits and fused agglomerates at high temperatures during combustion, resulting in the malfunctioning of combustion systems. Potassium, calcium, and silicate are the main metals which could contribute to agglomeration [47]. Due to this, both RS and CC need specific pretreatment before being used as fuel. It is recommended to cut corncobs into smaller pieces to decrease the moisture before carbonization in the kilns. Liu et al. [48] reported biochar washing with acetic acid and citric acid could decrease ash contents to mitigate the slagging and fouling issues.

3.5. Application of CH Biochar for Water Filtration

As CH biochar has better physical properties than the other biochars, particularly for the adsorption capability (highest iodine number), the CH biochar was selected to study its application as a filter media. The CH biochar was selected to study its application as a filter media for canal water filtration to reduce nutrient inputs into aquaculture ponds. Canal water near a coastal aquaculture farm was used since CH residue is easily sourced in the coastal aquaculture area. The initial concentrations of NH_4^+ , NO_3^- , TP, and COD in the canal water were 0.12 mgN/L , 0.34 mgN/L , 1.14 mgP/L , and 192 mg/L , respectively. The biochar filter removed a substantial amount of COD from the canal water with 95% removal over 30 min of operation (Figure 6a). In contrast, the sand filter could not remove NH_4^+ (Figure 6b), whereas NH_4^+ adsorption occurred in the biochar filter, resulting in an effluent concentration which met the Thai coastal water quality standard for aquaculture ($<0.10 \text{ mg/L}$) [48]. It was evident that TP could not be removed in the biochar filter during the first 200 min of operation as it was initially released from the biochar itself. Then, TP was gradually removed to 0.52 mgP/L . On the contrary, TP could be removed in the sand filter during the first 200 min of operation and was not removed afterwards. It was noticed that effluent pH values of biochar and sand filters were in the range of 8.18–8.37 and 7.18–7.70, respectively. At a pH in the 7.2–12.7 range, phosphorus in the form of HPO_4^{2-} and TP removal in the biochar filter was possibly achieved by precipitation with calcium as CaHPO_4 [49]. This can be confirmed from the high amount of soluble base cation in the coconut husk biochar. A high pH could enhance NH_4^+ removal as the biochar surfaces exhibited a negative charge, but it was not favorable to adsorb NO_3^- . Nitrogen removal (NH_4^+ and NO_3^-) could also be achieved by microbial degradation via nitrification/denitrification reactions. In the present study, biochar and sand filters could not lower NO_3^- and TP concentrations to less than 0.06 mgN/L and 0.045 mgP/L , respectively, at the recommended level of coastal water quality for aquaculture [50]. However, the guidelines of water quality for coastal aquaculture for marine shrimp hatchery and nursery for the concentration of NH_4^+ and NO_3^- , are less than 0.4 mg/L and 60 mg/L , and no guideline values for TP and COD are mandated [51].

According to the prior discussion, biochar contains volatile matter and metals, and thus its toxicity to seedlings was considered in order to evaluate the biochar suitability as a soil amendment. The Petri dish test method without soil was conducted as an easy and rapid ecotoxicological test for the initial screening of biochars used as a soil amendment [52]. It was found that the % GI of media after water filtration was significantly higher than virgin media ($p\text{-value} < 0.05$). The GI values of sand and CH biochar before water filtration were 49.0% and 46.2%, respectively, whereas the values were 90.2% and 132.9% for sand and biochar after water filtration, respectively (Figure 7). The % RE after water filtration was also significantly higher than virgin media ($p\text{-value} < 0.05$), while % RSG of media before and after water filtration was not significantly different at 0.05. The germination inhibition which occurred for virgin biochar was likely due to the elevated pH. The volatile organic compounds originating from the carbonization process could also inhibit seed germination [53]. Moreover, $\text{NH}_4^+\text{-N}$ can be a significant factor affecting phytotoxicity [22].

Biochar released NH_4^+ and it would be converted to unionized NH_3 by more than 80% at 30°C when it is exposed to a high pH_{soil} value of 9.75 [54]. In addition, the increment of GI and RE values implies that the adsorbed nutrients from the canal water could stimulate seed germination. Hence, using virgin biochar without mixing with soil may affect plant seedlings.

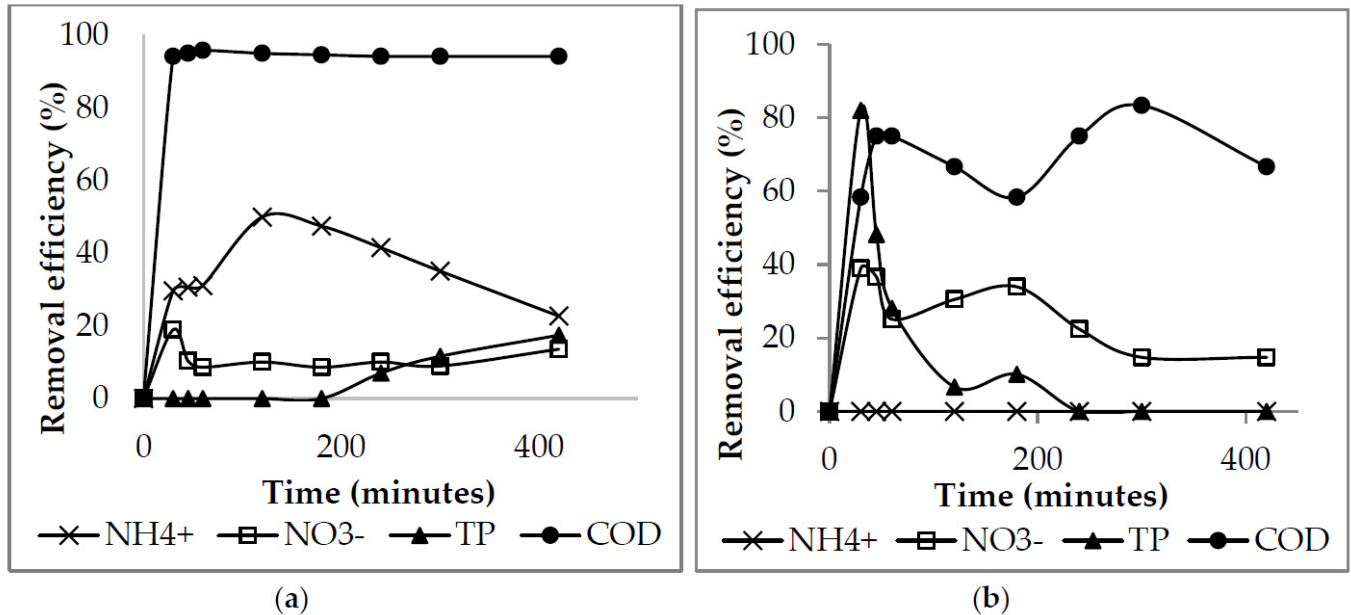


Figure 6. NH_4^+ , NO_3^- , TP and COD removal efficiencies by biochar and sand filters. (a) Biochar filter and (b) sand filter.

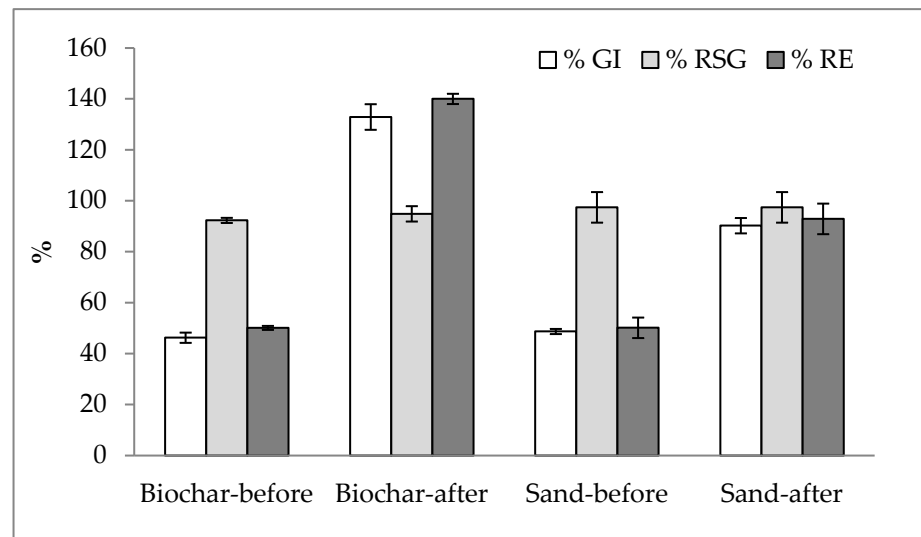


Figure 7. Percentage of GI, RSG, and RE for sand and biochar extracts.

4. Conclusions

The data presented in this study show that temperature in a drum kiln is related to the type of agricultural residues. Biochars from CH and CS residues can be used as fuel, for soil amendment, or as adsorbents since they have high heating value, high soluble N and P for plant growth, high acidic functional groups for cationic adsorption, and a high iodine number for pollutant adsorption in pores. CC biochar has high moisture, which is not suitable for fuel use, and has less surface functional groups for adsorption. Thus it would require either pretreatment or surface modification. Alternatively, it can be used as a soil amendment. Production of RS biochar by the horizontal kiln had a small yield

and high ash content, which is suitable for soil amendment for enhancing soil fertility. In addition, it can be used as adsorbent for cationic adsorption since it has high silica groups on its surfaces. CH biochar can be used as filter media for canal water treatment to improve water quality in coastal aquaculture, and the spent biochar can be applied to support the growth of plant seedlings.

Author Contributions: Conceptualization, S.V. and D.W.; funding acquisition, S.V. and D.W.; investigation, P.S.; methodology, R.N., T.T., B.P., P.S. and W.M.; project administration, S.V. and D.W.; supervision, B.P.; writing–review & editing, S.K., R.N., T.T., S.V., D.W. and W.M. All authors have read and agreed to the published version of the manuscript.

Funding: This research was funded by the Thailand research fund (TRF) no. RDG6030006, and by the Newton Fund via the Biotechnology and Biological Sciences Research Council (BBSRC) of the United Kingdom (BB/P027709/1).

Institutional Review Board Statement: Not applicable.

Informed Consent Statement: Not applicable.

Data Availability Statement: Not applicable.

Conflicts of Interest: The authors declare no conflict of interest.

References

1. Tun, M.M.; Juchelkova, D.; Win, M.M.; Thu, A.M.; Puchor, T. Biomass energy: A overview of biomass sources, energy potential, and management in Southeast Asian countries. *Resources* **2019**, *8*, 81. [CrossRef]
2. Wyn, H.K.; Zarate, S.; Carrascal, J.; Yerman, L. A novel approach to the production of biochar with improved fuel characteristics for biomass. *Waste Biomass Valorization* **2020**, *11*, 6467–6481. [CrossRef]
3. Ding, Y.; Liu, Y.; Liu, S.; Li, Z.; Tan, X.; Huang, X.; Zeng, G.; Zhou, L.; Zheng, B. Biochar to improve soil fertility. A review. *Agron. Sustain. Dev.* **2016**, *36*, 36. [CrossRef]
4. Lin, X.W.; Xie, Z.B.; Zheng, J.Y.; Liu, Q.; Bei, Q.C.; Zhu, J.G. Effect of biochar application on greenhouse gas emissions, carbon sequestration and crop growth in coastal saline soil. *Eur. J. Soil. Sci.* **2015**, *66*, 329–338. [CrossRef]
5. Fidel, R.B.; Laird, D.A.; Parkin, T.B. Effect of biochar on soil greenhouse gas emissions at the laboratory and field scales. *Soil Syst.* **2019**, *3*, 8. [CrossRef]
6. Boehm, A.B.; Bell, C.D.; Fitzgerald, N.J.M.; Gallo, E.; Higgins, C.P.; Hogue, T.S.; Luthy, R.G.; Portmann, A.C.; Ulrich, B.A.; Wolfand, J.M. Biochar-augmented biofilters to improve pollutant removal from stormwater-can they improve receiving water quality. *Environ. Sci. Water Res. Technol.* **2020**, *6*, 1520–1537. [CrossRef]
7. Chen, J.; Li, C.; Ristovski, Z.; Milic, A.; Gu, Y.; Islam, M.S.; Wang, S.; Hao, J.; Zhang, H.; He, C.; et al. A review of biomass burning: Emissions and impacts on air quality, health and climate in China. *Sci. Total Environ.* **2017**, *579*, 1000–1034. [CrossRef] [PubMed]
8. Kakareka, S.V.; Kukharchyk, T.I. PAH emission from the open burning of agricultural debris. *Sci. Total Environ.* **2003**, *308*, 257–261. [CrossRef]
9. Lewandowski, W.; Rym, M.; Kosakowski, W. Thermal biomass conversion: A review. *Processes* **2020**, *8*, 516. [CrossRef]
10. Sparrevik, M.; Field, J.L.; Martinsen, V.; Breedveld, G.D.; Cornelissen, G. Life cycle assessment to evaluate the environmental impact of biochar implementation in conservation agriculture in Zambia. *Environ. Sci. Technol.* **2013**, *47*, 1206–1215. [CrossRef]
11. Pangnakorn, U.; Watanasorn, S.; Kuntha, C.; Chuenchooklin, S. Application of wood vinegar to fermented liquid biofertilizer for organic agriculture on soybean. *Asian J. Food Agro-Ind.* **2009**, *2*, S189–S196.
12. Jindo, K.; Mizumoto, H.; Sawada, Y.; Sanchez-Monedero, M.A.; Sonoki, T. Physical and chemical characterization of biochars derived from different agricultural residues. *Biogeosciences* **2014**, *11*, 6613–6621. [CrossRef]
13. Guizani, C.; Jeguirim, M.; Valin, S.; Limousy, L.; Salvador, S. Biomass chars: The effects of pyrolysis conditions on their morphology, structure, chemical properties and reactivity. *Energies* **2017**, *10*, 796. [CrossRef]
14. Gwenzi, W.; Chaukura, N.; Noubactep, C.; Mukome, F.N.D. Biochar-based water treatment systems as a potential low-cost and sustainable technology for clean water provision. *J. Environ. Manag.* **2017**, *197*, 732–749. [CrossRef]
15. Ifa, L.; Yani, S.; Nurjannah, N.; Sabara, Z.; Yuliana, Y.; Kusuma, H.S.; Mahfud, M. Production of bio-briquette from biochar derived from pyrolysis of cashew nut waste. *Ecol. Environ. Conserv.* **2019**, *25*, S125–S131.
16. Tippayawong, K.Y.; Chaidi, N.; Ngamlertsappakit, T.; Tippayawong, N. Demand and cost analysis of agricultural residues utilized as biorenewable fuels for power generation. *Energy Rep.* **2020**, *6*, 1298–1302. [CrossRef]
17. Liu, Z.; Dugan, B.; Masiello, C.A.; Gonnermann, H.M. Biochar particle size shape, and porosity act together to influence soil water properties. *PLoS ONE* **2017**, *12*, 0179079. [CrossRef] [PubMed]
18. ASTM. *Standard Test Method for Determination of Iodine Number of Activated Carbon (D4607-94)*; ASTM International: West Conshohocken, PA, USA, 2021. Available online: <https://www.astm.org/Standards/D4607.htm> (accessed on 8 March 2021).

19. ASTM. *Standard Practice for Proximate Analysis of Coal and Coke (D3172-13)*; ASTM International: West Conshohocken, PA, USA, 2021. Available online: https://www.astm.org/DATABASE.CART/STD_REFERENCE/D3172.htm (accessed on 8 March 2021).
20. Yuan, J.H.; Xu, R.K.; Zhang, H. The forms of alkalis in the biochar produced from crop residues at different temperatures. *Bioresour. Technol.* **2011**, *101*, 3488–3497. [[CrossRef](#)] [[PubMed](#)]
21. APHA; AWWA; WEF. *Standard Methods for the Examination of Water and Wastewater*, 22nd ed.; American Public Health Association: Washington, DC, USA, 2012.
22. Tiquia, S. Reduction of compost phytotoxicity during the process of decomposition. *Chemosphere* **2010**, *79*, 506–512. [[CrossRef](#)]
23. Nafsun, A.I.; Herz, F.; Specht, E.; Scherer, V.; Wirtz, S. Heat Transfer Experiments in a Rotary Drum for a Variety of Granular Materials. *Exp. Heat Transf.* **2016**, *29*, 520–535. [[CrossRef](#)]
24. Cha, J.S.; Park, S.H.; Jung, S.-C.; Ryu, C.; Jeon, J.K.; Shin, M.C.; Park, Y.K. Production and utilization of biochar: A review. *J. Ind. Eng. Chem.* **2016**, *40*, 1–15. [[CrossRef](#)]
25. Lian, F.; Xing, B. Black carbon (biochar) in water/soil environments: Molecular structure, sorption, stability, and potential risk. *Environ. Sci. Technol.* **2017**, *51*, 13517–13532. [[CrossRef](#)]
26. Vassilev, S.V.; Baxter, D.; Vassileva, C.G. An overview of the behavior of biomass during combustion: Part I. Phase-mineral transformations of organic and inorganic matter. *Fuel* **2013**, *112*, 391–449. [[CrossRef](#)]
27. Garg, S.; Das, P. Microporous carbon from cashew nutshell pyrolytic biochar and its potential application as CO₂ adsorbent. *Biomass Convers. Biorefin.* **2020**, *10*, 1043–1061. [[CrossRef](#)]
28. Jouiad, M.; Al-Nofeli, N.; Khalifa, N.; Benyettou, F.; Yousef, L.F. Characteristics of slow pyrolysis biochars produced from rhodes grass and fronds of edible date palm. *J. Anal. Appl. Pyrolysis* **2015**, *11*, 183–190. [[CrossRef](#)]
29. Juhola, A.J. Iodine adsorption and structure of activated carbons. *Carbon* **1975**, *13*, 437–442. [[CrossRef](#)]
30. Mianowski, A.; Owczarek, M.; Marecka, A. Surface area of activated carbon determined by the iodine adsorption number. *Energy Sources Part A Recover. Util. Environ. Eff.* **2007**, *29*, 839–850. [[CrossRef](#)]
31. Xing, X.; Fan, F.; Jiang, W. Characteristic of biochar pellets from corn straw under different pyrolysis temperatures. *R. Soc. Open Sci.* **2018**, *5*, 172346. [[CrossRef](#)]
32. Domingues, R.R.; Trugilho, P.F.; Silva, C.A.; de Melo, I.C.N.A.; Melo, L.C.A.; Magriotis, Z.M.; Sanchez-Monedero, M.A. Properties of biochar derived from wood and high nutrient biomasses with the aim of agronomic and environmental benefits. *PLoS ONE* **2017**, *12*, 0176884. [[CrossRef](#)]
33. Collett, C.; Masek, O.; Razali, N.; McGregor, J. Influence of biochar composition and source material on catalytic performance: The carboxylation of glycerol with CO₂ as a case study. *Catalysts* **2020**, *10*, 1067. [[CrossRef](#)]
34. Sarfaraz, Q.; Silva, L.; Drescher, G.; Zafar, M.; Severo, F.; Kokkonen, A.; Molin, G.; Shafi, M.; Shafique, Q.; Solaiman, Z. Characterization and carbon mineralization of biochars produced from different animal manures and plant residues. *Sci. Rep.* **2020**, *10*, 955. [[CrossRef](#)]
35. Li, H.; Dong, X.; da Silva, E.B.; de Oliveira, L.M.; Chen, Y.; Ma, L.Q. Mechanisms of metal sorption by biochars: Biochar characteristics and modifications. *Chemosphere* **2017**, *178*, 466–478. [[CrossRef](#)]
36. Praspaliauskas, M.; Pedisius, N.; Cepauskiene, D.; Valantinavicius, M. Study of chemical composition of agricultural residues from various agro-mass types. *Biomass Convers. Biorefin.* **2019**, *10*, 937–948. [[CrossRef](#)]
37. Tubana, B.S.; Babu, T.; Datnoff, L.E. A review of silicon in soils and plants and its role in US agriculture: History and future perspectives. *Soil Sci.* **2016**, *181*, 393–411. [[CrossRef](#)]
38. El-Hassanin, A.; Samak, M.R.; Radwan, S.R.; El-Chaghaby, G.A. Preparation and characterization of biochar from rice straw and its application in soil remediation. *Environ. Nat. Resour. J.* **2020**, *18*, 283–289. [[CrossRef](#)]
39. Gonzalez, M.I.S.; Mackowiak, C.; de Almeida, A.Q.; de Carvalho Junior, J.I.T.; Andrade, K.R. Positive and negative effects of biochar from coconut husks, orange bagasse and pine wood chips on maize (*Zea mays* L.) growth and nutrition. *Catena* **2018**, *162*, 414–420. [[CrossRef](#)]
40. Wang, Q.; Sarkar, J. Pyrolysis behaviors of waste coconut shell and husk biomasses. *Int. J. Energy Prod. Manag.* **2018**, *3*, 34–43. [[CrossRef](#)]
41. Demirbas, A. Relationships between heating value and lignin, moisture, ash and extractive contents of biomass fuels. *Energy Explor. Exploit.* **2002**, *20*, 105–111. [[CrossRef](#)]
42. Demirbas, A. Relationships between lignin contents and heating values of biomass. *Energy Convers. Manag.* **2001**, *42*, 183–188. [[CrossRef](#)]
43. Zhang, X.; Yang, W.; Blasiak, W. Modeling study of woody biomass: Interactions of cellulose, hemicellulose and lignin. *Energy Fuels* **2011**, *25*, 4786–4795. [[CrossRef](#)]
44. Crombie, K.; Masek, O.; Sohi, S.P.; Brownsort, P.; Cross, A. The effect of pyrolysis conditions on biochar stability as determined by three methods. *Glob. Chang. Biol. Bioenergy* **2013**, *5*, 122–131. [[CrossRef](#)]
45. EBC. *European Biochar Certificate Guidelines for a Sustainable Production of Biochar*; European Biochar Foundation (EBC): Arbaz, Switzerland, 2019. Available online: <http://www.european-biochar.org/en/download10.13140/RG.2.1.4658.7043> (accessed on 5 January 2021).
46. TISI. *Community Product Standards*; TCPS Briquette Charcoal No. 238/2547; Community Product Standards Division, Thai Industrial Standards Institute: Bangkok, Thailand, 2004. (In Thai)

47. Teixeira, P.; Lopes, H.; Gulyurtlu, I.; Lapa, N.; Abelha, P. Evaluation of slagging and fouling tendency during biomass co-firing with coal in a fluidized bed. *Biomass Bioenergy* **2012**, *39*, 192–203. [[CrossRef](#)]
48. Liu, Z.; Hoekman, S.K.; Balasubramanian, R.; Zhang, F.S. Improvement of fuel qualities of solid fuel biochars by washing treatment. *Fuel Process. Technol.* **2015**, *134*, 130–135. [[CrossRef](#)]
49. Choi, Y.K.; Jang, H.M.; Kan, E.; Wallace, A.R.; Sun, W. Adsorption of phosphate in water on a novel calcium hydroxide-coated dairy manure derived biochar. *Environ. Eng. Res.* **2019**, *24*, 434–442. [[CrossRef](#)]
50. PCD. *Coastal Water Quality Standard*; Pollution Control Department: Bangkok, Thailand, 2021. Available online: http://pcd.go.th/info_serv/reg_std_water02.html (accessed on 8 March 2021).
51. ACFS. Good Aquaculture Practices for Marine Shrimp Hatchery and Nursery, Thailand Agricultural Standard, TAS 7422-2010. National Bureau of Agriculture Commodity and Food Standards, Ministry of Agriculture and Cooperatives. Available online: https://www.acfs.go.th/standard/download/eng/marine_shrimp_hatchery.pdf (accessed on 8 February 2021).
52. Rajalakshmi, A.; Kumar, S.K.; Bharathi, C.D.; Karthika, R.; Divya, V.K.; Meera, R.; Mohanapriya, S. Effect of Biochar in Seed Germination-in-vitro Study. *Int. J. Biosci. Nanosci.* **2015**, *2*, 132–136.
53. Mumme, J.; Getz, J.; Prasad, M.; Lüder, U.; Kern, J.; Mašek, O.; Buss, W. Toxicity screening of biochar-mineral composites using germination tests. *Chemosphere* **2018**, *207*, 91–100. [[CrossRef](#)]
54. Gray, N.F. Chapter 6-Water Pollution. In *Water Technology*, 2nd ed.; Gray, N.F., Ed.; Butterworth-Heinemann: Oxford, UK, 2005; pp. 87–112.